3-24-2006

Prototype and Testing of a MEMS Microcooler Based on Magnetocaloric Effect

Simone L. Ghirlanda
University of South Florida

Prototype and Testing of a MEMS Microcooler Based on Magnetocaloric Effect

by

Simone L. Ghirlanda

A thesis submitted in partial fulfillment
of the requirements for the degree of
Master of Science in Electrical Engineering
Department of Electrical Engineering
College of Engineering
University of South Florida

Major Professor: Shekhar Bhansali, Ph.D.
Muhammad Rahman, Ph.D.
Sangchae Kim, Ph.D.
Elias (Lee) Stefanakos, Ph.D.

Date of Approval:
March 24, 2006

Keywords: magnetic refrigeration, magnetic materials, gadolinium, permanent magnet, adiabatic demagnetization

To my family

ACKNOWLEDGMENTS

My advisor, Shekhar Bhansali, has been the source of inspiration and guidance throughout my graduate career. None of my success would have been possible without his efforts to teach me how to test, present, and articulate ideas.

I am also most grateful to my family in Italy: my parents who spent many years of my childhood inspiring me with life goals and teaching me about the value of education, who have shown their true love by allowing me to pursue my university studies away from home, and who have always been so close to me even from the other side of the ocean; my sister Ilaria who I have always been able to count on whenever I needed; both of my grandmothers for their affection and phone calls; my uncle Alberto who has often talked to me and given me suggestions about the engineering professional life; and both of my grandfathers and great aunts who I wish could have still been here today to share this moment.

My sincere gratitude goes to my beautiful girlfriend Amy who has always been there for me with love, support and motivation for these past four years across two states. I would also like to acknowledge my “second family” in Texas, Alan and Kaye Ostermann along with Lisa, Nathan and Seth who gave me the opportunity to come live in the US for a year during high school and continue to be an important part of my life today.

I would also like to thank everyone directly involved with the MEMS Microcooler Project at University of South Florida. In particular I am grateful to Senthil

Sambandam, Luis Rosario, Bharath Bethala, and Shantanu Shevade, for having the courage to initiate such a project. Sang Chae Kim deserves great credit for acting as lead researcher and keeping the project afloat during this past year and a half. The project's only undergraduate student volunteer, Carl Adams, also deserves my sincere appreciation for helping to make my ideas a reality as well as giving precious suggestions.

I am also thankful to those who have provided friendship, support, and/or inspiration including Stephen Bates, Eddie Bettega, Roberto Cuneo, Matteo Fossati, Francesco Martinelli, Federico Mautone, Paolo Migliavacca, Federico Pippo, Marco Pollastri, Tony Price, Tony Rosado, Riccardo Signorelli, Omar Souza, Rodrigo Trejos and Silvia Volpini.

I am thankful as well for the support and guidance of my committee, Muhammad Rahman, Sang Chae Kim, and Elias Stefanakos of University of South Florida. I also wish to acknowledge the inspiration for graduate studies given to me at my Alma Mater, The University of Texas at Austin, in particular by Professors Brian Evans, Thomas Milner, Theodore Rappaport, and Baxter Womack of the ECE Department.

Finally, I wish to thank all those in the BioMEMS and Microsystems Lab who have made this thesis more than just a single person's research project. I am very thankful for all the feedback I have received from them. In particular, I wish to thank Shyam Aravamudhan, Subramanian Krishnan, Kevin Luongo, Joe Register, Praveen Sekhar, Altagrace Sine and Andrew Farmer of the Center for Ocean Technology.

This research was supported by NASA under the grant "Hydrogen Research at Florida Universities (HYRES)".

SIMONE L. GHIRLANDA

University of South Florida, May 2006

TABLE OF CONTENTS

LIST OF TABLES

LIST OF FIGURES

PROTOTYPE AND TESTING OF A MEMS MICROCOOLER BASED ON MAGNETOCALORIC EFFECT

Simone L. Ghirlanda

ABSTRACT

This thesis documents the work and research effort on the design, fabrication and testing of a magnetocaloric MEMS microcooler, focusing on the testing of the microcooler at low magnetic fields. The phenomenon of magnetocaloric effect (MCE), or adiabatic temperature change, which is obtained by heating or cooling magnetic materials due to a varying magnetic field, can be exploited in the area of magnetic refrigeration as a reliable, energy-efficient cooling system. In particular, its applications are being explored primarily in cryogenic technologies as a viable process for the liquefaction of hydrogen. The challenge for magnetic refrigeration is that the necessary MCE is most easily achieved with high magnetic fields (5-6 Tesla) provided by superconducting magnets. However, a significant magnetocaloric effect can be exhibited at lower magnetic fields (1-2 Tesla) by carefully controlling initial temperature conditions as well as by selecting, preparing and synthesizing the optimal fabrication process of Silicon (Si) wafers. A microcooler was integrated based on previous works of others and tested. Finally, testing of the magnetocaloric effect was conducted and results analyzed. Experimental results in these domains demonstrate that magnetic refrigeration can be part of the best current cooling technology, without having to use volatile, environmentally hazardous fluids. The MEMS magnetocaloric refrigerator demonstrated a ~ -12º C change in the temperature of cooling fluid at a magnetic field of 1.2 T.

CHAPTER 1 INTRODUCTION

The fundamental motivation of magnetocaloric refrigeration is to study alternative solutions for more efficient liquefaction of hydrogen. Generally this type of refrigeration requires the use of superconducting magnets able to produce strong magnetic fields in the range of 4-6 Tesla (T) as well as the use of ferromagnetic compounds based on rare earth elements such as gadolinium (Gd). However, superconducting magnets are very expensive and require extensive servicing which ultimately defeats the purpose of finding an efficient alternative type of refrigeration. The primary advantages of this cycle are its relatively high cost-effectiveness ratio and environment friendliness.

MEMS Microcoolers are proposed as a solution to the challenge of reducing magnetic fields: with MEMS coolers using just permanent or electro-magnets in the magnetic field range of only ~1 T would be feasible, as (a) they provide a large surface area for a given volume; (b) they reduce the pole to pole distance resulting in adequate field intensity. In addition, MEMS Microcoolers add flexibility not only in the liquefaction of hydrogen, but in other real-world scenarios, such as household refrigeration and air-conditioning systems. Such small systems can also be used for Zero Boil-Off (ZBO) control.

Sophisticated non-hazardous refrigeration systems are difficult to implement, in part because they are likely to be extremely complex, perhaps requiring the synthesis and optimization of hundreds of different forms of magnetocaloric materials with optimal properties. This thesis describes a method for implementing a sophisticated and effective magnetocaloric refrigerator by preparation of

magnetocaloric material GdSiGe, design and development of micro-fabrication processes for prototype micro-coolers and validation of the model with experimental results.

This chapter begins by presenting the motivation for magnetocaloric micro-refrigeration, then briefly describes the approach and concludes with an overview of the results and contributions of the thesis.

1.1 Motivation

Magnetic refrigeration has shown great promise as a viable process for liquefaction of hydrogen. It is a potentially compact, reliable and efficient technology whose qualities are highlighted by the absence of hazardous or environmentally damaging chemicals (such as chlorofluorocarbons). Additionally, it is “up to 60%” efficient (based on the temperature of operation). On the other hand today’s best commercial devices (vapor-compression refrigerators), which basically extract heat from a vapor using a compressor, achieve a maximum efficiency of about 40% [1].

Magnetic refrigeration can also be useful for heat dissipation in Zero Boil-Off (ZBO) cryogenic storage vessels. The miniaturization of this effective refrigeration system could be a key technology for future Pico-satellites. Also, because of its small size and lightweight it could be used to re-liquefy hydrogen in cryogenic storage tanks used for transportation and storage of hydrogen for space missions.

In magnetocaloric refrigeration, the effectiveness is measured in terms of the (a) cooling-capacity / magnetic-field ratio and (b) the volume of liquid extracting heat from (or dissipating it to) the ferromagnetic material in the least amount of time possible. In this regard, a miniaturized magnetocaloric cooling system with a Silicon (Si) microstructure is needed when not using superconducting magnets. The use of MEMS technology enhances the surface area to volume ratio, improving the heat

transfer between the fluid and the ferromagnetic material, and enables the magnetic poles to be close to each other, resulting in greater field intensity. The improved heat transfer, with reduced distance between poles, enables operating at low magnetic field.

This approach presents a pathway to evaluate inexpensive and environment-friendly solutions to difficult vapor compression refrigeration technology. It can even lead to common household refrigeration systems that can obtain competitive results utilizing permanent magnets. Such a system is developed and evaluated in this thesis.

1.2 Approach

Ferromagnetic materials heat up or cool down when inserted into a varying magnetic field. The second law of thermodynamics states that the entropy (or disorder) of a closed system must increase with time. This is known as magnetocaloric effect (MCE) and it was originally discovered in iron by Warburg [2]. The MCE is intrinsic to all magnetic materials and is due to the coupling of the magnetic sub-lattice with the magnetic field, which reduces the spin entropy in the ferromagnetic material. This results in the alignment of the electron spins in the atoms of the material with the direction of the magnetic field. To compensate for the effect and keep the process adiabatic (i.e. the total entropy of the system remains constant during the magnetic field change) the conservation of total entropy leads to the enhancement of lattice entropy (i.e. the motion of the atoms becomes more random), thus raising the temperature of the material. In the case of a magnetic refrigerator, the heat would be absorbed by liquid (or air) flowing in the ferromagnetic material. Once the magnetic field is removed, the spin entropy is enhanced again and, the temperature of the material falls below that of its environment. This allows it to draw more unwanted heat, resulting in the cool down of liquid (or air) flowing in the

refrigerant material. In other words, just as the compression of a gas, the isothermal magnetizing of a ferromagnetic material reduces its entropy, while vice-versa, demagnetizing (comparable to the expansion of a gas) restores the zero-field entropy of a system [2].

Designing and developing a valid “alternative” form of magnetic refrigeration presents several technical challenges in order to match current technology: the heating and cooling efficiency provided by existent MCE refrigerators is usually highly dependent on the size of the applied magnetic field as well as the magnetic moments which tend to be largest in rare-earth elements. This would generally require the use of superconducting magnets (expensive and requiring extensive maintenance). The goal for the microcooler is to eliminate the use of such magnets with no loss in cooling capability and, at a moderate cost without the use of environmentally hazardous chemicals.

The MEMS microcooler meets these challenges through four technical optimizations: (1) preparation of magnetocaloric material GdSiGe and its synthesis in different forms with optimal properties; (2) design and development of microfabrication processes for prototype microcoolers based on Silicon microstructure; (3) exploiting the peak of entropy of the compound at significant low temperature; and (4) building an experimental setup to validate the concept. These conditions work together in optimizing solutions as part of the refrigeration process. This approach results in high cooling capability that can be adopted for the uses described above as a valid alternative to current existing technology, and also makes entirely new applications possible.

1.3 Contributions and Impact

The main contribution of this thesis is developing a MCE system to validate magneto-caloric refrigeration, under low magnetic fields, as a viable process for liquefaction of hydrogen. Several experiments, conducted in the research, demonstrate the feasibility of an effective MEMS microcooler based on magnetocaloric effect at a low magnetic field, and others suggest how the approach could be used for real-world applications such as a household refrigerator.

First, the properties of magnetocaloric material GdSiGe and its synthesis in different forms were studied by *S.N. Sambandam et al* [3]. In particular, the peaks of entropy of this compound are analyzed to come to the conclusion that significant MCE results can be obtained even at low magnetic field if working at significant low temperatures.

Second, the design, development and testing of micro-fabrication process for prototype micro-coolers was undertaken and is described elsewhere [4]. By analysis of previous research project in the same area, it is clear that one challenge is to be able to design and realize a system at the small scale level. This thesis presents integration and testing of the microcooler. Several experiments were undertaken to validate individual concepts that ultimately led to the assembly of a micro-cooler significantly smaller in size compared to what is currently available. By exploiting the dimensions of the device, it is possible to obtain a remarkable MCE at a significantly low magnetic field (~ 1.2 T). The microcooler presented a challenge to its system analysis because in-situ temperature sensors are needed to be integrated in the system in order to validate and model the experimental results. This had been done in related research [5].

The key driver for these experiments is high cooling capacity. Interestingly, the MEMS microcooler succeeds in obtaining a discrete MCE utilizing an electro-magnet capable of producing a magnetic field of less than 1.5 T. This is a first step towards a better alternative to conventional vapor compression refrigeration technology as well as household refrigeration, and opens up exciting avenues for future research.

1.4 Overview of the Thesis

The thesis is divided into four parts: Literature Review (Chapter 2), System Set-Up and Specifications (Chapter 3), Testing and Results (Chapter 4), and Conclusion (Chapter 5).

Chapter 2 reviews the history of application of the magnetocaloric effect and prior work in magnetocaloric refrigeration.

Chapter 3 presents a detailed description of the experiment settings and the system integration including electro-magnet, GdSiGe block, Silicon wafer, syringe pump, cooling chamber, bonding procedure, and temperature sensors.

Chapter 4 focuses on the testing procedures undertaken to characterize the performance of the MEMS microcooler as well as discussion of the results obtained.

Chapter 5 discusses and reviews the major contributions of the MEMS microcooler and ideas for future research.

CHAPTER 2 LITERATURE REVIEW OF MAGNETIC REFRIGERATION

This chapter will review the history of continuous magnetic refrigeration and previous application work resulting in an active magnetic regenerator cycle. After briefly reviewing specifications and settings of the experiment, the results and discussion of it are presented. Finally, the chapter concludes with a review of issues in competitive magnetic refrigeration that the MEMS microcooler attempts to address.

2.1 History of Continuous Magnetic Refrigeration

The history of continuous magnetic refrigeration goes back to the work of Collins and Zimmerman [6], and Heer [7]. They were the first ones to build and test magnetic refrigerators operating between 0.2 K - 0.73~1 K by continuously magnetizing and demagnetizing iron ammonium alum. Their latest system (in 1953) was able to extract 12.3 μJ/s from the cold reservoir at 0.2 K operating at 1/120 Hz frequency. However, few years had to pass before Brown [8] was able to realize a near room temperature continuously operating magnetic refrigerator. To accomplish this result, studies were conducted to explore magnetic refrigeration properties at significantly higher temperatures. This allowed scientists to conclude that a much larger temperature span was possible. Brown was able to attain a 47 Celsius no-load temperature difference between the hot inlet (46º C) and cold outlet (-1º C) flowing a combination of water and alcohol into a magnetocaloric bed made in Gd with a magnetic field change of 0 to 7 T. Following the early work of Brown, two other scientists, Steyert [9] and Barclay [10, 11], continued with design and development of the concept of active magnetic regenerator (AMR) refrigeration which was

successively brought to life in several experiments at different temperatures. One of these experiments performed by *Zimm et al.* [12] is described below.

2.2 Near-Room Temperature Magnetic Refrigerator

Magnetic refrigeration is based on the magnetocaloric effect (MCE). In the case of ferromagnetic materials, the MCE corresponds to a warming as the magnetic moments of the atoms are aligned by the application of the magnetic field and vice-versa upon removal of the magnetic field.

This paper reviews the description and performance of a near-room temperature magnetic refrigerator developed at the Astronautics Technology Center in Madison, WI based on previous similar work done at Ames Laboratory of Iowa State University. The unique aspect of the research is that it uses the active magnetic regeneration concept of recent cryogenic devices, but in contrast to the cryogenic case, the heat capacity of the fluid in the pores of the regenerator bed is compared to that of the solid matrix.

The magnetic warming and cooling generated by the magnetocaloric effect can present almost no losses in soft ferromagnets such as gadolinium (Gd) based compounds, allowing for the possibility of an extremely efficient refrigeration process. There are two major challenges in the design of a refrigerator based on magnetocaloric effect. First, unless a strong magnetic field is applied (5 T or more) the magnetocaloric effect (MCE) is fairly small. Even with an optimal material such as gadolinium, a maximum adiabatic temperature change of 11º K can be produced. Second, as the ferromagnetic material is a solid, it is not easy to pump it through heat exchangers, as in the case for gas and vapor cycle refrigerants.

This second problem however can easily be solved by utilizing a heat transfer fluid, such as water, and regeneration (full cycle) can be obtained by flowing it

through a porous bed of magnetocaloric material which is alternatively magnetized and demagnetized by respectively inserting it and removing it from the applied magnetic field.

In this case an Active Magnetic Regenerator Refrigerator (AMRR) was chosen, in which the magnetocaloric bed generates refrigeration that appears to regenerate the bed itself using the thermal linkage of the fluid. This particular version requires that the heat capacity of the fluid is much less than that of the bed so that the temperature gradient remains in the magnetocaloric bed. At first, the use of water as the heat transfer fluid seemed problematic, as water trapped in the pores of a bed of gadolinium spherical particles has a capacity equal to that of the refrigerant material. However, the volume of water flown through the bed was held to less than that of the pore volume. This overcame the problem and a successful device could be designed on this basis.

The AMRR tested (schematically shown in Figure 2.1) is made of two 1.5 kg beds composed of Gd spheres. The magnetic field is provided by conventional liquid helium immersed NbTi solenoid mounted in a warm bore dewar. The two magnetocaloric beds are alternatively inserted in the magnetic field of 1-5 T using an air cylinder drive. The magnetic refrigerant material used in the experiment was gadolinium metal and it was only 93% pure.

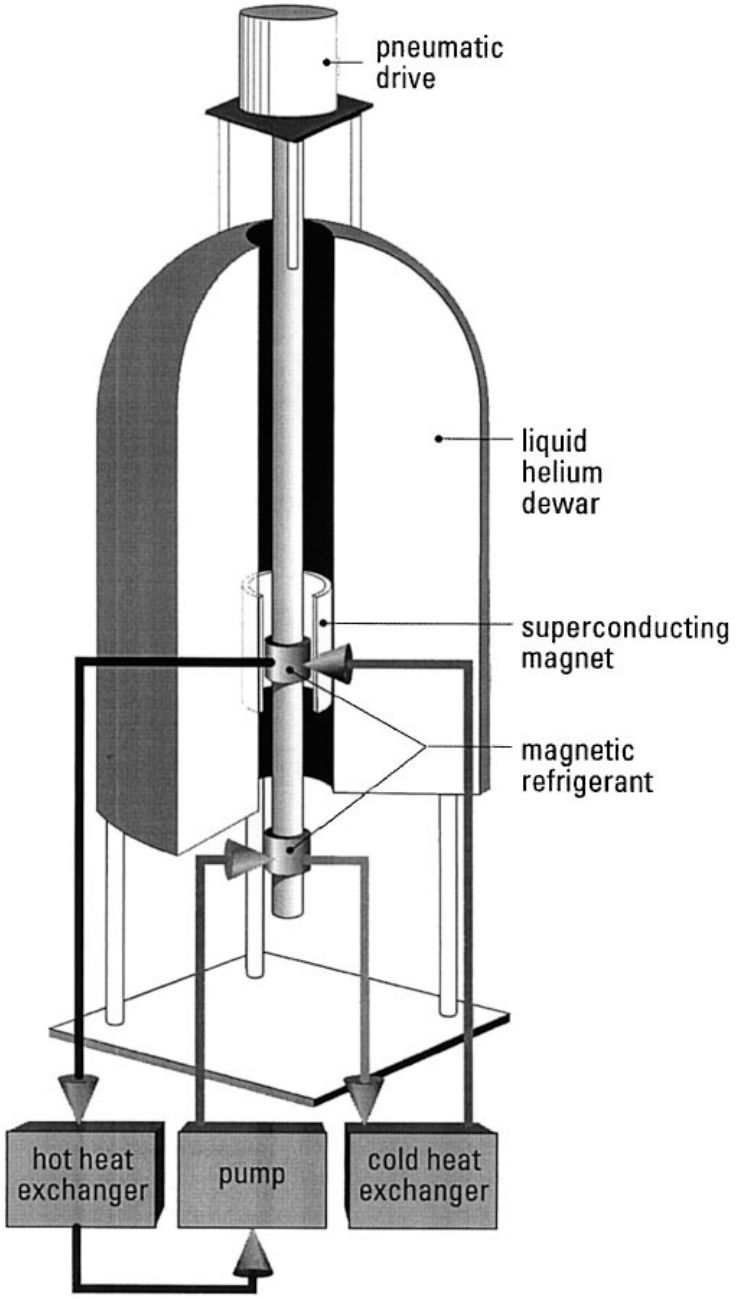

Figure 2.1 A schematic sketch of the AMR refrigerator[9]

The flow starts in a primary loop with fluid being cooled as it passes through the demagnetized bed. Next, the water picks up a thermal load by passing through the cold heat exchanger (CHEX). Heat then is extracted while the water is flown through the hot heat exchanger (HHEX) and returns to the pump inlet. After a standard time interval, the magnetized bed is removed from the magnetic field to let the demagnetized one's insertion. At this point the flow direction is reversed and the

thermal load supplied to the CHEX by a secondary flow loop. The heat is removed from the HHEX by a secondary flow path using cooling water. Temperatures were measured at the inlet and outlet of each heat exchanger as well as inside each magnetocaloric beds in five locations.

As expected, the cooling power is proportional to the magnetic field increase throughout the cycle and initially it is also proportional to the fluid flow rate. However, a decrease in cooling power is also expected with increasing temperature because the adiabatic temperature change of gadolinium decreases with temperature below its Curie point [12].

In conclusion, as expected, a considerable temperature change and cooling effect of 12º K was obtained only at a high magnetic field (5 T). Up to 600 W of cooling power was generated in a 5 T magnetic field while only 200 W of cooling power was produced at 1.5 T. The efficiency of the system approaches 60% at 5 T (while only 30% at 1.5 T) of Carnot. However, this didn't take into account the power used to load the superconducting magnet.

2.3 Conclusion

The AMR cycle described above has several positive features useful for practical application in the area of magnetic refrigeration [2]. First, since the MCE of each individual particle of the magnetocaloric bed changes the entire temperature profile across the bed itself, the temperature span of a single stage can easily exceed that of the whole magnetic refrigerant. Second, because the bed is composed by particles which ultimately together act as their own generator, heat doesn't need to be transferred between two separate solid assemblies, but rather only between each solid particle within the same bed via the action of a fluid. Third, since the individual particles in the bed do not encounter the entire temperature span of the stage, the

magnetocaloric bed can be prepared into layers of different magnetic material which ultimately could be optimized depending on the particular temperature range.

However, the results obtained above, particularly in terms of temperature span, are substantial only at a high magnetic field (5 T), which requires the use of superconducting magnets. Therefore, although the work done gives a good insight on magnetic refrigeration, the current system makes the idea an unpractical alternative to current near-room refrigeration systems, such as household refrigerators, and the air conditioning market. This combined with the characteristics of the refrigerant material used, Gd, and the potential for very high efficiency inspires further research in the area.

CHAPTER 3 SYSTEM SET-UP AND SPECIFICATIONS

This chapter focuses on all the work done prior to the experiment. In particular it gives details about the electro-magnet used, the refrigerant material synthesis, the fabrication of the Silicon wafer, the syringe pump as well as the details of the experiment set-up such as cooling chamber and temperature sensors integration. The overall system set-up is presented in Figure 3.1.

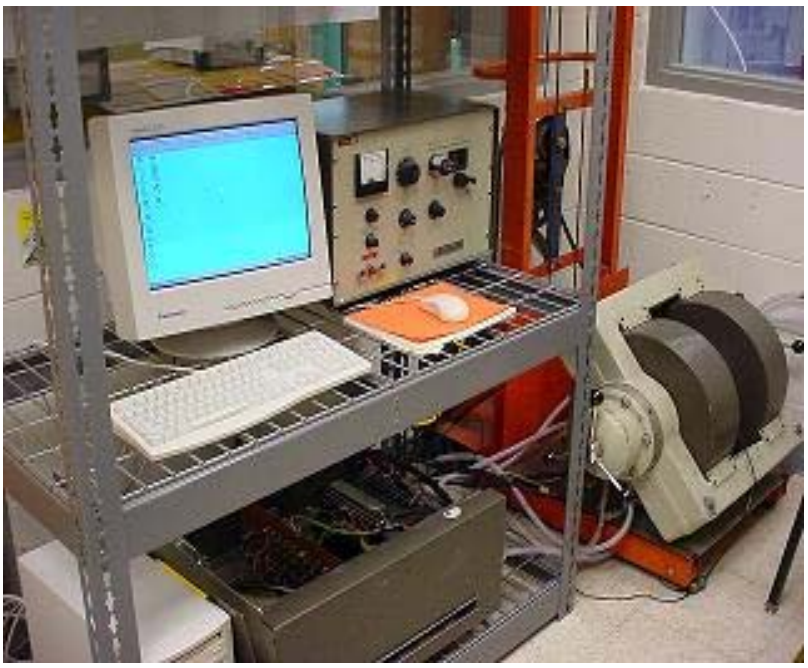

Figure 3.1 Experimental setup for refrigeration testing

3.1 Magnet Specifications

As stated earlier, one major difference in this project from past works in magnetic refrigeration, where superconducting magnets are usually the popular choice, is that an electro-magnet was selected to be used. This choice was made for

two main reasons. First, because as it was seen before, the use of superconducting magnets is not feasible as a choice for current household refrigeration or air conditioning systems because of its large size, high cost and extensive servicing requirements. Second, because an electro-magnet was available at no cost as part of the equipment of the Department of Electrical Engineering and given its magnetic field capacity of up to ~ 1.7 T, it should be possible to simulate the effect of a permanent magnet which would be the ultimate solution to create a technology able to compete with current existent devices. Low energy requirements would be crucial to create a winning alternative technology, therefore the choice to produce a system capable of operating with permanent magnets.

The magnet utilized in the experiment is a Varian electro-magnet with magnetic field capability of up to ~1.7 T. The main transformer enables approximately 42 A of current to charge two spiral coils, one in each magnetic disc and the magnetic field is created. The controller uses a feedback loop which relies on a Hall probe to be able to maintain the magnetic field at certain strength without unnecessary oscillations which could be caused by external agents.

3.1.1 Magnetic Field Measurements

Several measurements were done on the magnetic field alone to get more precise data and correlate the distance of the poles to the magnetic field produced. The maximum magnetic field is about 1.2 T at a gap of approximately 3 cm. This was about the minimum space needed in order to perform the experiment. It was established that the magnetic field drastically decreases with increasing pole to pole distance. Figure 3.2 shows the magnetic field measurements as a function of distance between poles.

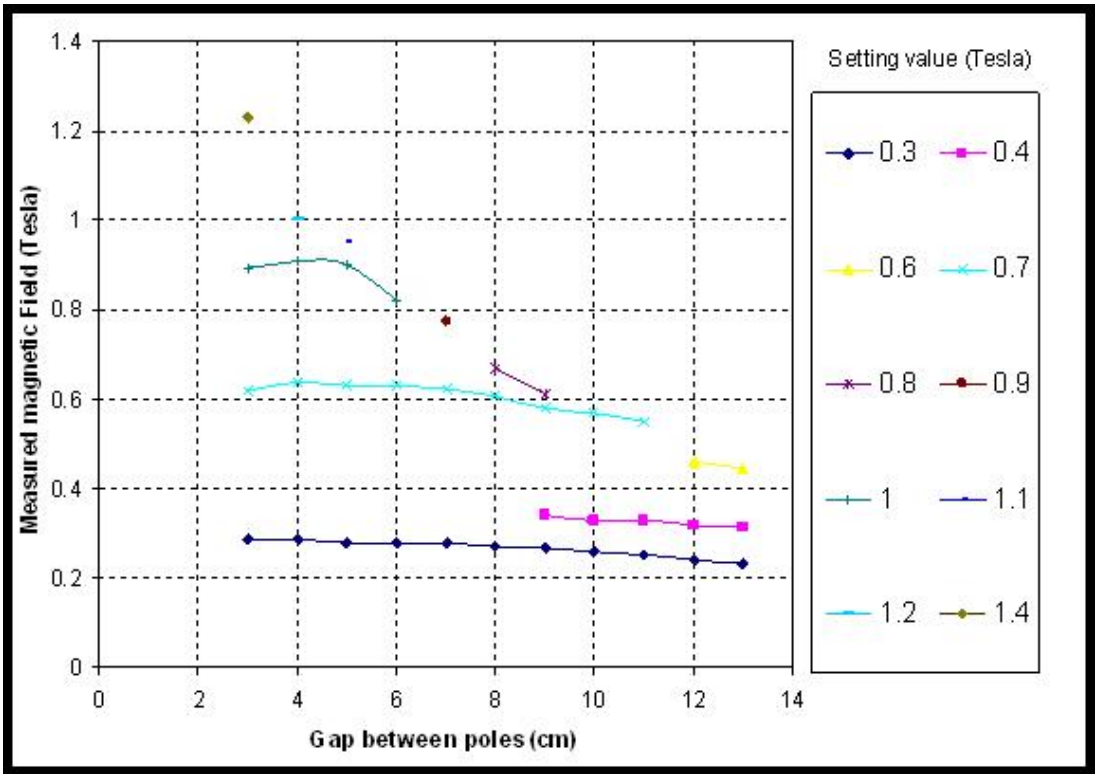

Figure 3.2 Magnetic field vs. distance between poles

At a distance of about 2 cm the poles are pulled together by the magnetic field strength. Also, any material interfering with the field seems to decrease the strength of it. Different materials such as plastic, sponge, and cardboard were tested in order to optimize the preparation of a cooling chamber which would interfere as little as possible with the magnetic field. Table 3.1 presents the results.

Table 3.1 Effect of materials interfering with the magnetic field

Surrounding Type	Magnetic field without box (Tesla)	Magnetic field in the box (Tesla)
Plastic box	0.925	0.865
Plastic Box + Sponge	0.925	0.77
Card board/ Styrofoam	0.925	0.905

As it can be seen from the table both plastic and sponge drastically decrease the magnetic field, while only cardboard and Styrofoam have a slight effect on it. This insight lead the idea of building a cooling chamber made in Styrofoam.

3.2 GdSiGe Block Specifications and Testing

As described by *S.N. Sambandam et al.* [3] GdSiGe alloys were synthesized at the Ames Laboratory of Iowa State University by preparing mixtures of Gd (99.8% purity), Si and Ge (both 99.99% purity). The mixture was arc melted in an argon atmosphere on a water cooled copper hearth. Each mixture was re-melted at least six times. The resulting alloy button was turned over after each melting to achieve alloy homogeneity. The mass of the mixtures was chosen not to exceed 25 g to achieve highest possible solidification and cooling rates, and the last melting step was always terminated by shutting down the power to the arc. All alloys are initially examined for any impurity phases, and those that possess monoclinic crystal structure were heat treated at 1570 K for one hour. The heat treatment was carried out in vacuum using an induction furnace. The alloy buttons were wrapped in Ta foils to avoid any kind of oxidation in the furnace. After the heat treatment, the alloys were rapidly cooled by shutting down the power of the induction coil. These alloy buttons were then grounded and powdered. The powder was then compacted using room temperature iso-static pressing to yield the 2 inch diameter discs [13].

3.2.1 GdSiGe Block Properties

Initially, studies and research were undertaken to better understand the GdSiGe block magnetocaloric properties at different initial temperature values. The synthesized powders of GdSiGe were characterized for magnetic and magnetocaloric properties. The dependence of magnetization of GdSiGe on temperature at a magnetic

field strength of 5 Gauss was measured and is plotted in Figure 3.3. It shows a paramagnetic to ferromagnetic transition between 260º K and 300º K. This indicates that the material is magnetic and has two composite phases that undergo transition.

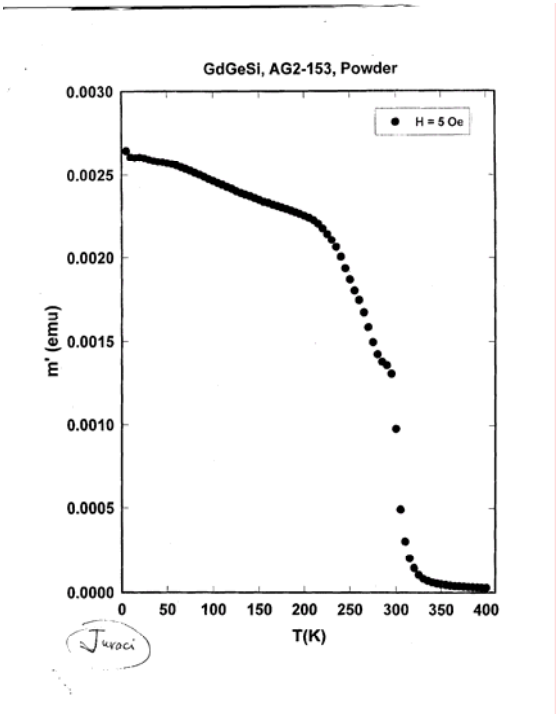

Figure 3.3 Magnetization with temperature for GdSiGe disc

The magnetocaloric effect has been studied and is shown in Figure 3.3 by the plot of change in magnetic entropy with temperature, indicating maximum magnetic entropy change at the transition temperatures. This has been accomplished by indirectly measuring entropy change from heat capacity measurements. Heat capacity measurements have been made on the samples from 240 K to 300 K at different applied magnetic fields from 1 T to 5 T (10 kOe to 50 kOe). The magnetic entropy can be deduced using the following Eq. (1) [13],

$$\Delta S(T,\Delta H) = \int_0^{T_c} \frac{C(T,H_2) - C(T,H_1)}{T} dT$$

where C(T, B) and C(T, 0) are the values of heat capacity in field B and in zero field, T being the temperature. It has earlier been demonstrated that this method yields comparable results derived from magnetization measurements [14].

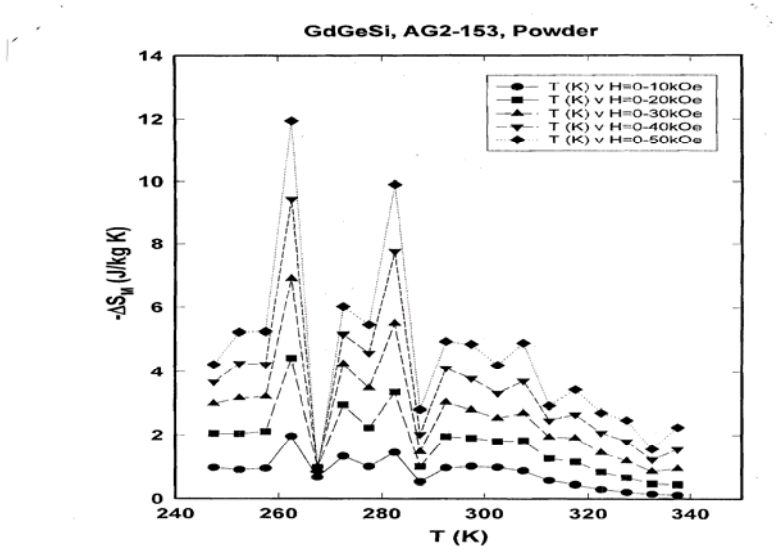

Figure 3.4 Magnetic entropy changes for GdSiGe disc at various magnetic fields

Figure 3.4 shows the entropy change calculated from the heat capacity measurements over a temperature range of 240º K to 340º K for varying applied magnetic fields from 1 to 5 Tesla. The peak of entropy change is observed near 262º K and 280º K.

3.2.2 Cooling Chamber

A cooling chamber built in Styrofoam between the magnet poles was prepared utilizing metal plates on each side and on the top which were frozen by pouring liquid nitrogen. However, holes were cut through the chamber around the poles to completely expose them so that the magnetic field wouldn't get affected by the Styrofoam. This allowed controlling the temperature inside the chamber and the initial

temperature of the GdSiGe block, keeping it stable for an extended period of time. Furthermore, tests were performed with the magnet being switched on and off to make sure this alone didn't affect the temperature in the chamber when no GdSiGe block is exposed to the magnetic field. The cooling chamber set-up is shown in Figure 3.5.

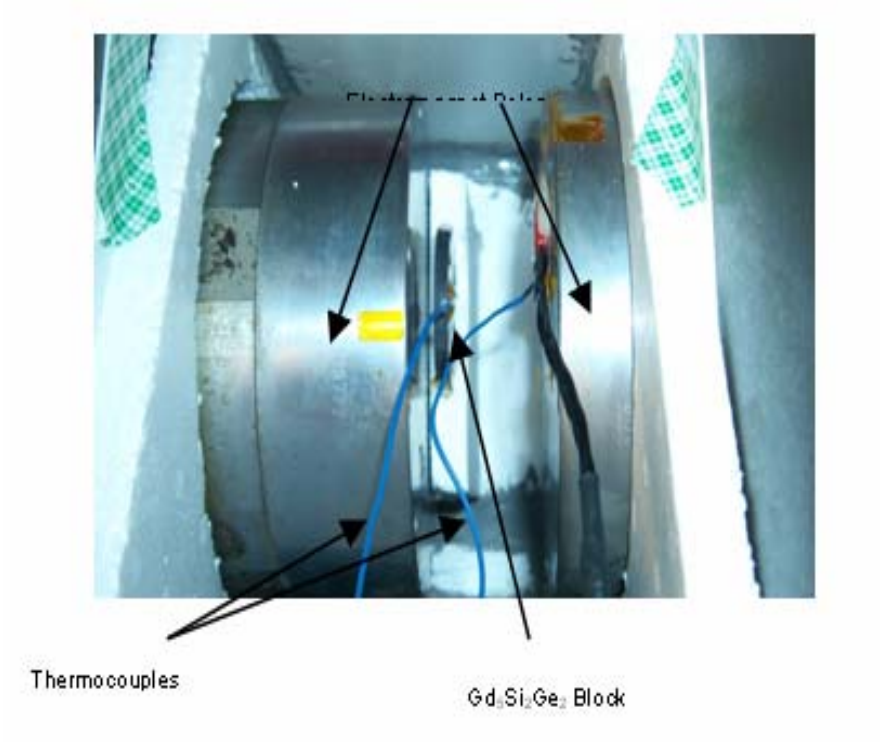

Figure 3.5 Cooling chamber around magnetic poles

3.2.3 GdSiGe Block Testing

Changes in temperature were recorded in the GdSiGe block at an applied magnetic field of approximately 1.2 Tesla. More precisely, the peaks of entropy change described in Figure 3.4 were taken into account when performing the testing procedure. Beginning at low temperatures (-16º C), a stable magnetic field of 1.2 T was applied directly to the GdSiGe block for approximately 90 seconds. It took

approximately 30 seconds for the electro-magnet to reach a maximum output of ~42 A. The temperature change was measured using a thermocouple, which has a 0.1° C resolution, through which data was logged every second. As a result in Figure 3.6, the GdSiGe block initial temperature of -16º C rose to – 9º C. This is because the entropy of the block reduces, as the fields align themselves, in presence of magnetic field thus dissipating heat. Successively, when the magnet was switched off and the magnetic field removed, demagnetization occurred and the block temperature dropped to -12º C within approximately a minute and stabilized at that temperature. This resulted because the entropy of the block increases by absorbing heat. The effect can be used for cooling of fluids in the microchannels. It was noticed that the increase and decrease in temperature was not equal due to the heat, which was generated, from the increasing stage. Similar testing was performed at -10º C, -6.5º C, 1.5º C, 4.5º C, and 7º C. However, as observed from Figure 3.6, changes of temperature progressively attenuated for higher initial temperatures. These results can be correlated with Figure 3.4, which shows the entropy change. Entropy change peak as shown in Fig. 3.4 exists at 262º K (-11º C), and the maximum temperature change of the block is observed around that peak in Fig. 3.7. Though an entropy change peak exists at 280º K (7º C), no appreciable temperature change was observed. This was due to the applied 1.2 T magnetic field, whose peak of entropy is observed only near 262º K. At higher magnetic fields, there would be appreciable temperature change around 280º K.

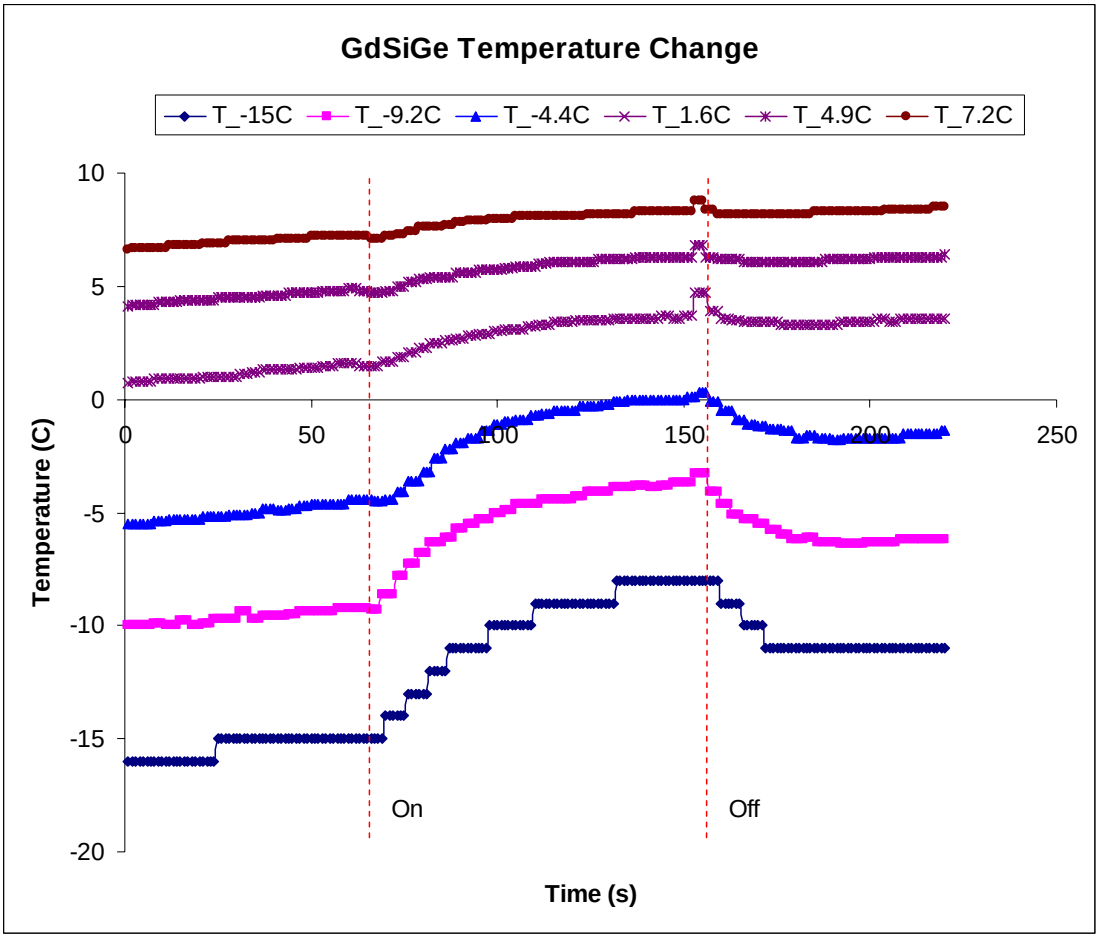

Figure 3.6 MCE at different initial temperatures

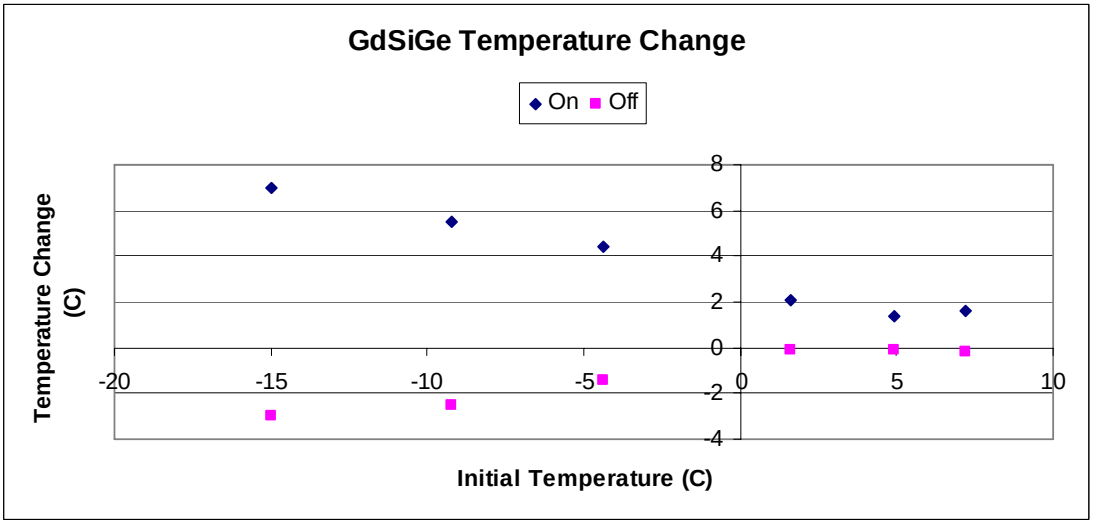

Figure 3.7 GdSiGe Temperature Change

3.3 Design of Microcooler

As described in *S.C. Kim et al.* [4], the design of the microcooler is schematically shown in Figure 3.8. Eight fluidic micro-channels of trapezoidal shape, each 300 µm wide, 150 µm deep and 25 mm long were fabricated in a 1 inch × 1 inch area on a 2 inch silicon (100) wafer. The micro-channels were designed to ensure an adequate mass of GdSiGe dedicated for cooling. The channels had a minimal spacing of 2700 µm between them.

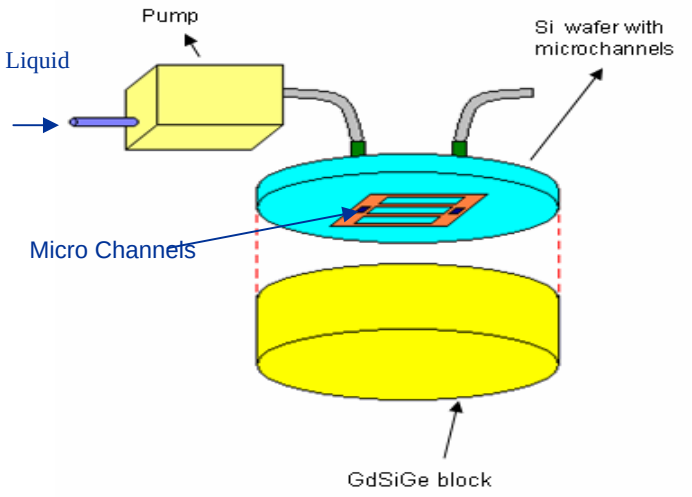

Figure 3.8 Design of the microcooler

Microconnectors were attached to the inlet and outlet ports of the wafer with microchannels as shown in Figure 3.9. The wafer was then attached to a 2 inch, 5 mm thick GdSiGe block using crystalbond TM 509. The adhesive was dissolved in acetone and sprayed on the GdSiGe surface, which was then allowed to evaporate resulting in a 4~5 µm thin uniform layer of adhesive. The thickness of the resultant adhesive layer was dependent on the initial mixture of the adhesive and acetone [4].

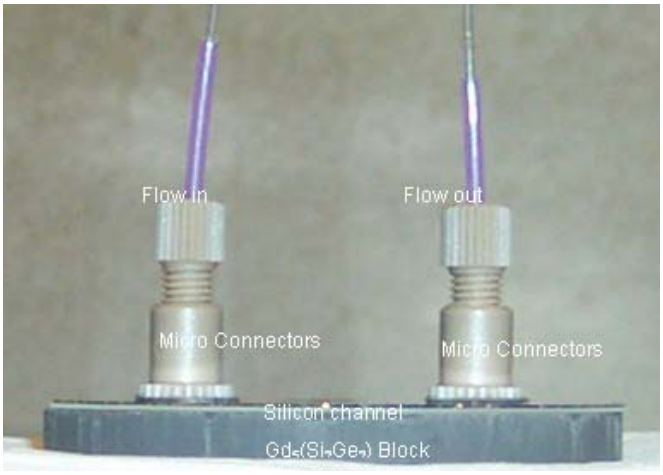

Figure 3.9 Microconnectors

The fabricated microchannels are shown in Figure 3.10 and 3.11 [4].

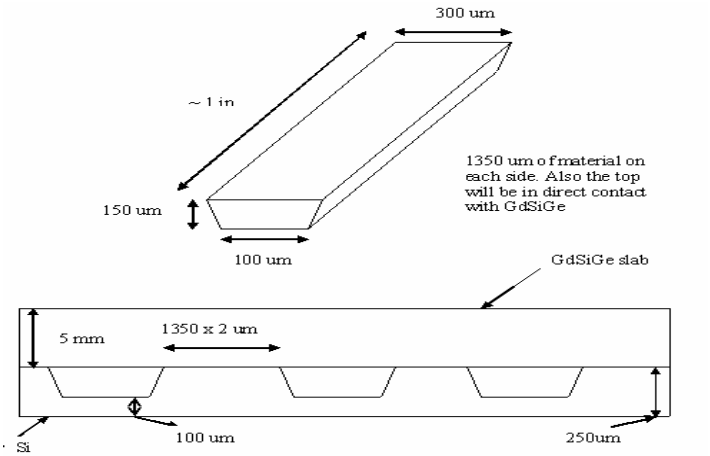

Figure 3.10 Prototype of microcooling channels

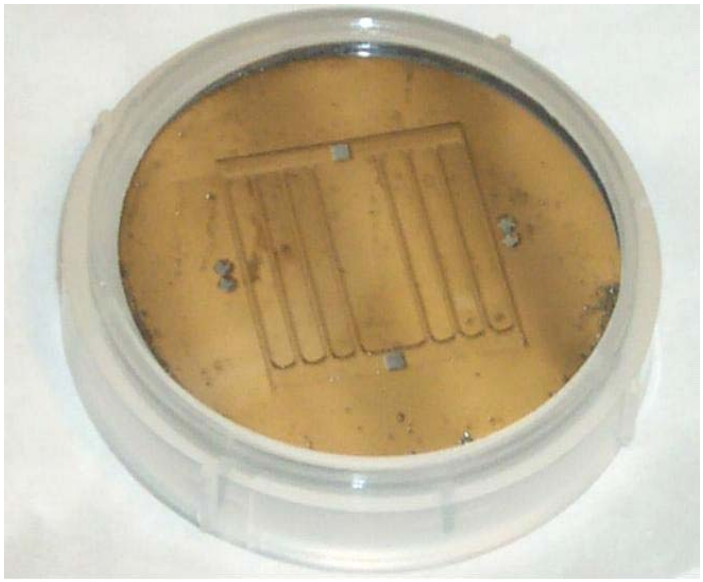

Figure 3.11 Eight micro channels fabricated on a Si wafer

3.3.1 Wafer-to-Wafer Bonding

Wafer-to-wafer bonding was a necessary last step needed to seal the face of created micro channels and be able to collect data when running fluid through the microchannels. Several ways to perform Si-to-Si wafer bonding were explored to ensure that the bond would withstand the low testing temperature. They consisted primarily in the use of (a) super-glue, (b) potassium silicate, and (c) crystal bond materials. However, none of them were strong enough to prevent leaking from occurring when testing the flowing of fluids such as water or anti-freeze through the microchannels. The high pressure caused by the syringe pump, even at the slowest possible rate of flow, seemed to be too much for the different type of bonding materials to handle. Finally, anodic bonding and fusion bonding were explored.

3.3.1.1 Anodic Bonding

Anodic bonding is a process which permits the sealing of a silicon wafer to a glass one. The two wafers are assembled and heated on a hot plate in a room atmosphere to

temperature between 400-500 deg. A high voltage and low current DC power supply is connected to the assembly such that the silicon is positive with respect the glass. Then by applying ~1.5 kV across the assembly for about 20 minutes, the glass seals to the metal. Figure 3.12 shows a drawing of the experimental setup.

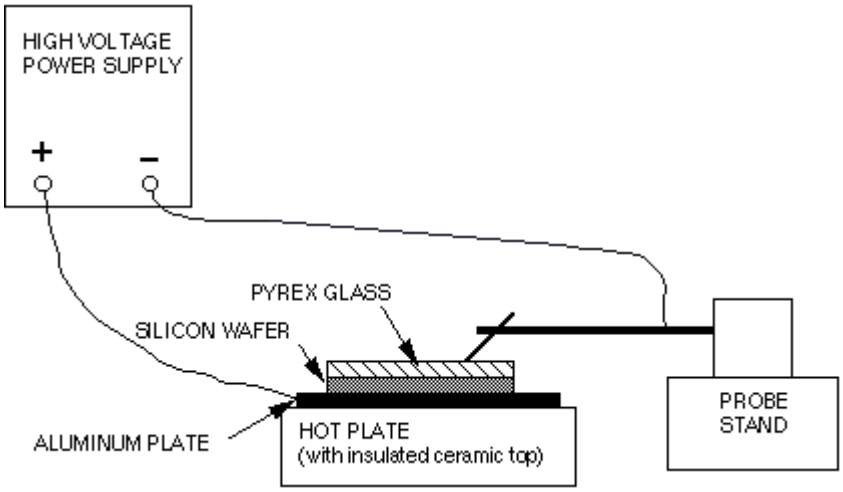

Figure 3.12 Schematic diagram of the experimental setup for anodic bonding

During the process, the positive Na ions in the glass are thermally excited resulting in increased mobility and in their attraction to the negative electrode on the glass surface. This causes their removal. The stronger bound negative ions in the glass form a space charge layer adjacent to the silicon surface. Initially the potential is uniformly distributed across the glass, but after the positive sodium ions have drifted toward the surface a large potential drop occurs at the glass/anode interface. The resulting electric field between the surfaces pulls them into contact. This causes the bonding to begin below the negative electrode and to spread across the surface. At the end of the process, the wafers are held together by a chemical bond which is irreversible [15].

3.3.1.2 Fusion Bonding

In fusion bonding, the substrates are first forced into intimate contact by applying a high contact force. Once in contact, the substrates hold together due to atomic attraction forces (Van der Waal), which are strong enough to allow the bonded substrates to be handled. The substrates are then placed in a furnace and annealed at high temperature, after which a solid bond is formed between the substrates.

3.3.2 Syringe Pump

In order to perform the fluid flowing part of the experiment a syringe pump was used. The CAVRO XP 3000 uses a stepper-motor driven syringe and valve design to aspirate and dispense measured quantities of liquid. Both the syringe and the valve are replaceable.

The syringe plunger is moved within the syringe barrel by a rack and pinion drive that incorporates a 1.8 degrees stepper motor and quadrature encoder to detect lost steps. The syringe drive has a 30 mm travel length and resolution of 3000 steps (3000 or 24000 steps for microstep-enabled firmware). The top of the syringe barrel attaches to the pump valve by a 1/4-28" fitting which is the size of the micro-tubes used for the flowing of liquid.

3.3.3 Temperature Sensors Integration

In order to be able to monitor temperature on the wafer’s inlet and outlet, digital temperature sensors were used. However, because of their size they could not be integrated directly into the wafer. Therefore, a small rectangular piece of Plexiglas was used in order to create a “temperature recording center”. Two small channels were drilled through the Plexiglas while temperature sensors were also inserted into the same channels by drilling holes from the other face of the rectangle. Micro-

connectors were attached on both sides so that liquid could flow directly from the wafer into the Plexiglas and temperature could be recorded without disturbing the cycle.

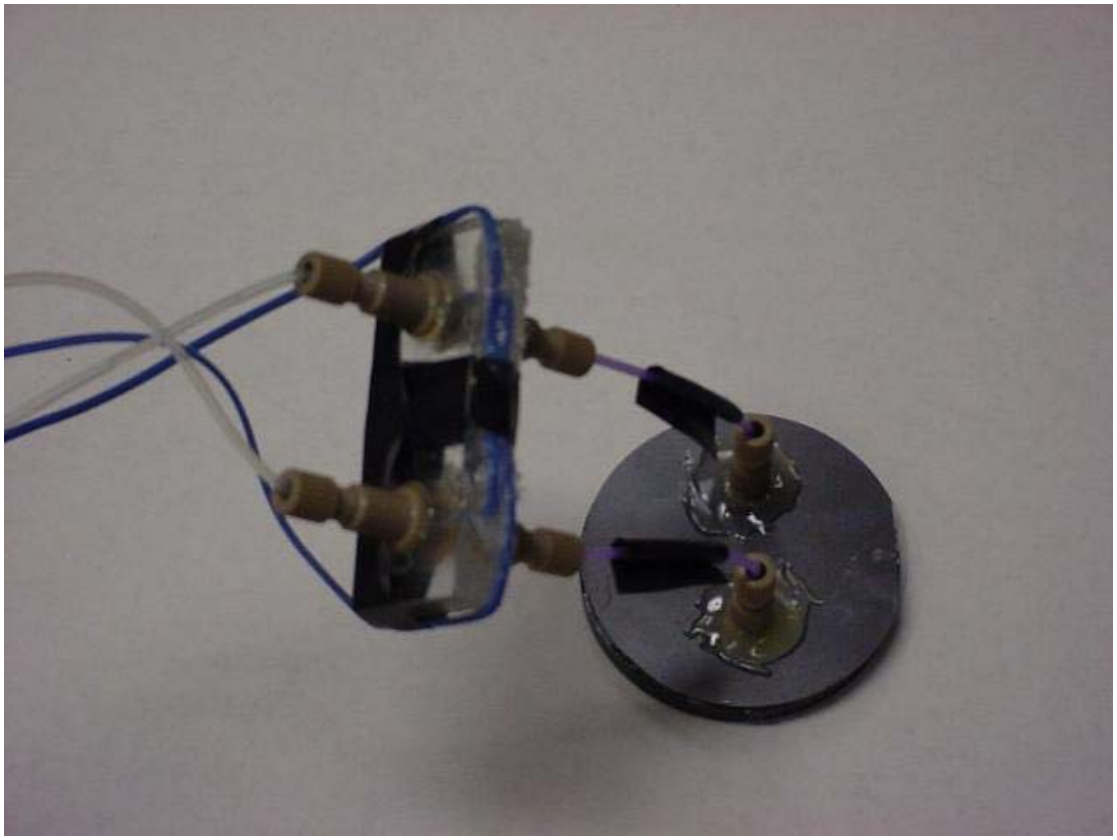

Figure 3.13 Temperature Sensors' Integration

CHAPTER 4 TESTING AND RESULTS

This chapter will review the testing procedure and results obtained as well as the future work inspired by the project. First a “Plexiglas wafer” was used in order to analyze only the effect of the refrigerant material itself. Then Silicon wafer results are presented both for the anodic bonding case which uses Si-to-Glass as well as for the fusion bonding case which allows the use of Si-to-Si. Finally, discussion and comparison of the results take place and ideas for future work are briefly presented.

4.1 Plexiglas “Dummy” Wafer Testing and Results

During the first liquid testing procedure, a “dummy” wafer made in Plexiglas (an insulator) was chosen to be used. This choice allowed testing of only the cooling properties of the GdSiGe block without it being influenced by the conducting effect of Silicon (while wafer-to-wafer bonding solutions were explored). A small channel was created on the bottom surface of a small rectangular Plexiglas block and this was mounted on top of the GdSiGe sample so that the liquid could be flowing in contact with the sample itself. A mixture of anti-freeze and water was used as fluid in this experiment since initial system temperature was below 0 C. A syringe-pump with a 5.0 ml capacity was used in order to flow the solution through the channel. The coolant was pumped at a rate of 5 ml/min. That corresponds to a flow rate of about 83.3 μL/s. The Plexiglas wafer is shown in Figure 4.1.

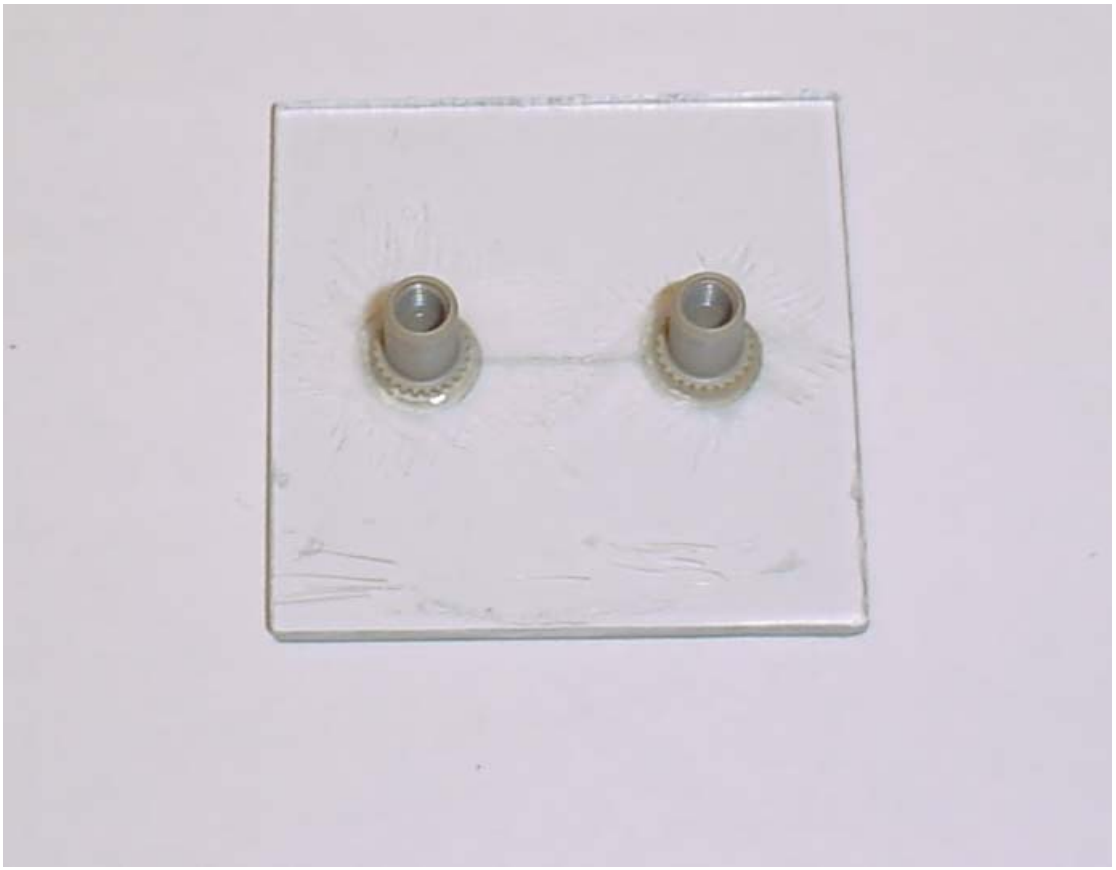

Figure 4.1 Plexiglas Wafer

The graph in Figure 4.2 describes the sensors' response of changing temperature versus time at constant magnetic field. The initial temperature was stabilized around the peak of entropy change previously analyzed and found at -11 C for GdSiGe. The outlet liquid temperature was normalized with the inlet liquid temperature at magnet off in order to study the results of the magnetic effect itself and not the results of the GdSiGe block being at an initial cold temperature.

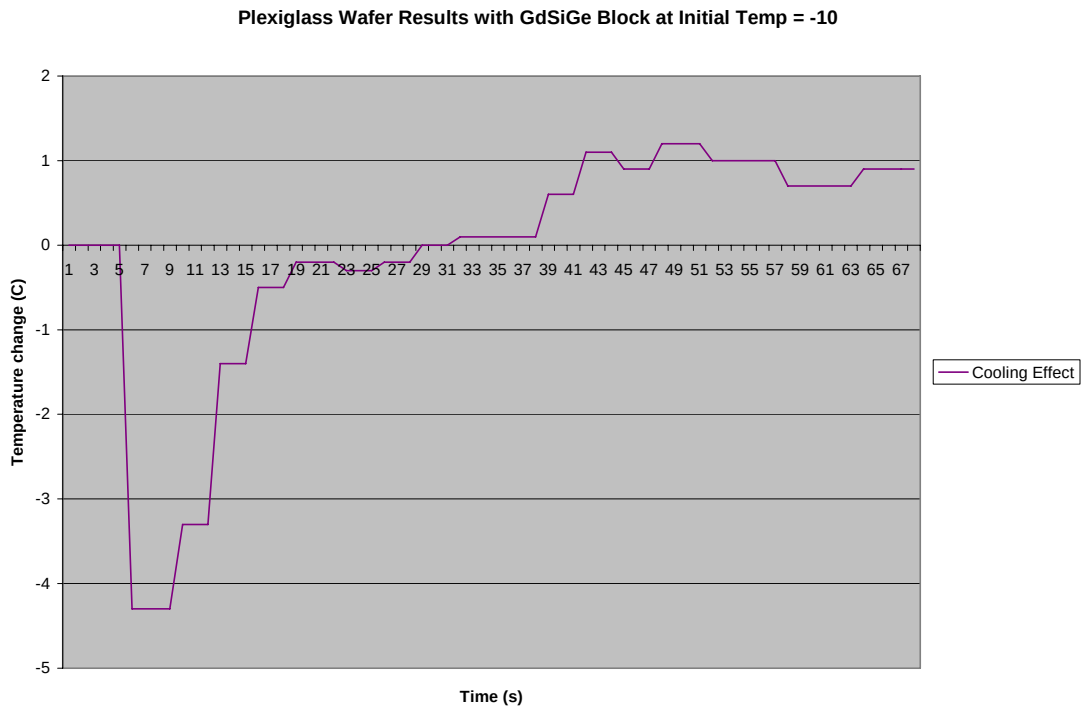

Figure 4.2 Plexiglas Wafer Results at Initial Temp. of -10 C

During the first few seconds of the process the magnet was off. However, inlet liquid temperature was below zero as a result of the residual liquid left into the micro-tube and the preparation of the cooling chamber through the use of liquid nitrogen which brought the liquid temperature below 0 C. This time however was used to make the adjustment needed on the outlet temperature to avoid consideration of the cooling process caused by the GdSiGe block itself kept at -10 C. In the plot, the first few seconds present a steep drop in temperature (of over 4 C) which is the result of demagnetization (since the magnet had been turned on shortly before). The magnet was turned on after approximately 10 seconds. At that point the inlet liquid temperature as expected began increasing. After approximately another 10 seconds the effect of magnetic heating began becoming evident. It takes roughly 20 seconds for the magnet to reach its full magnetic field capacity of ~1.2 T. As observed from the same plot, in this case, at the ideal starting temperature of -10 C, the heating

process led to a temperature change of about 5 C (from -4C to +1C). As we'll see in the next section, this was improved by the use of a Silicon wafer exploiting its heat conducting properties.

4.2 Silicon Wafer Testing

The second part of the experiment was conducted on a real Silicon wafer which is an excellent thermal conductor. Both the anodic bonding version (which presented a Glass wafer to Silicon wafer combination mounted on top of the GdSiGe block) and the fusion bonding one (Silicon wafer to Silicon wafer mounted on top of GdSiGe block) were tested. These two solutions were expected to produce better results than the ones obtained by the Plexiglas wafer because Silicon is a good heat conductor. In order to prevent excessive pressure which ultimately could cause leaks, a lower flow rate of 33.3 μL/s was chosen. This would allow a testing procedure of about 2 minutes and 30 seconds to take place. First, liquid nitrogen was used to obtain the desired initial temperature conditions. Then, once the system temperature had stabilized, the mixture of water and anti-freeze would flow through the system for about 10 seconds in order to eliminate all residual liquid left into the tubes and microchannels whose temperature would be affected by the overall chamber initial conditions. This would ensure that any new change in temperature in the system should be attributed only and exclusively to the varying magnetic field and not to other causes. At approximately 10 seconds, the magnet was turned on to reach its maximum output (~1.2 T) in about 20 seconds, while liquid still flew through the system at a constant rate. Once reached its maximum output capability (indicated by the controller reaching 42 A), the magnet was left on for 10 seconds for magnetization and then off /demagnetization for the rest of the time since the cooling effect was the ultimate interest in the experiment. Another important aspect to take into account is

that the GdSiGe block is sealed and placed far from where the liquid nitrogen was poured, therefore any change in temperature following the initial temperature system stability must be only due to the changing magnetic field.

4.2.1 Results for Silicon-to-Glass

The testing of Si-to-Glass combination was analyzed in several sessions. Beginning at a temperature of about 5º C, the first testing session was performed and the results are presented in Figure 4.3. The plot of temperature vs. time shows the response of the sensors on liquid flowing into a Si-to-Glass wafer combination.

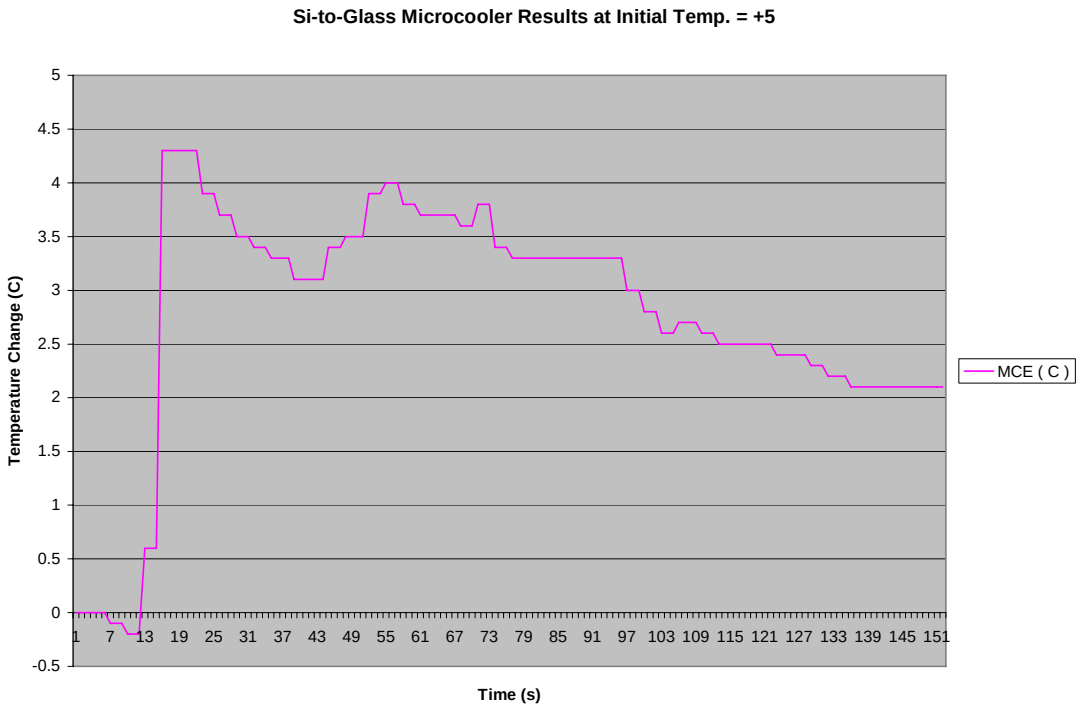

Figure 4.3 Si-to-Glass Microcooler at Initial Temp. of +5 C

As it is observed from the figure, a slight cooling effect is noticeable. In particular, as the magnet was turned on and maximum magnetic field capacity reached after approximately 20 seconds, a heating “burst” is evident on the excel

graph (over 4º C). This is because GdSiGe is not a continuous heat source but an instantaneous one. However, because far from the ideal initial condition temperature of -11º C (change of entropy peak) as seen before, no actual cooling effect is provided once the magnet was turned off (demagnetization) but only an attenuation of the heating effect. This effect is strictly due to demagnetization as the process was started once the initial temperature had stabilized to approximately 5º C (and no more liquid nitrogen was provided during the process), therefore, if anything, the overall chamber temperature condition could slightly increase with time but definitely not decrease except because of the MCE caused by the magnetic field applied on the GdSiGe block.

As the experiment was repeated, with initial temperature conditions lowered to about 3º C and the same exact procedure took place, a further decrease in heating effect during demagnetization was recorder as presented in Figure 4.4. However, this change in fluid temperature does not correspond to a true “cooling” effect yet either but more to a strong weakening of the heating moment. That again can only be attributed to the demagnetization process since no more liquid nitrogen was added during the process.

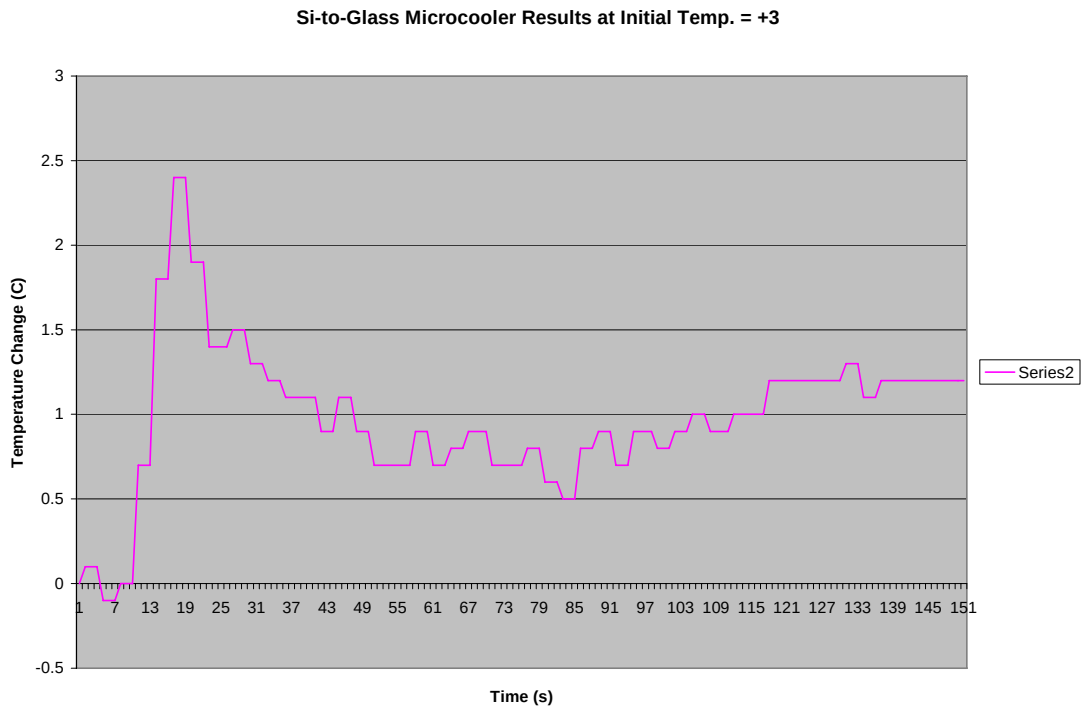

Figure 4.4 Si-to-Glass Microcooler at Initial Temp. of +3 C

Continuing in the experiment procedure, initial system temperature condition was lowered to about 1º C. After a usual heating peak appearing at around 20 seconds into the experiment (magnet at full capacity), the magnet was turned off as in the previous case. However, this time a slight true "cooling effect" took place with almost a 1º change (at outlet) below the fluid temperature measured at the microcooler inlet. Figure 4.5 presents the results.

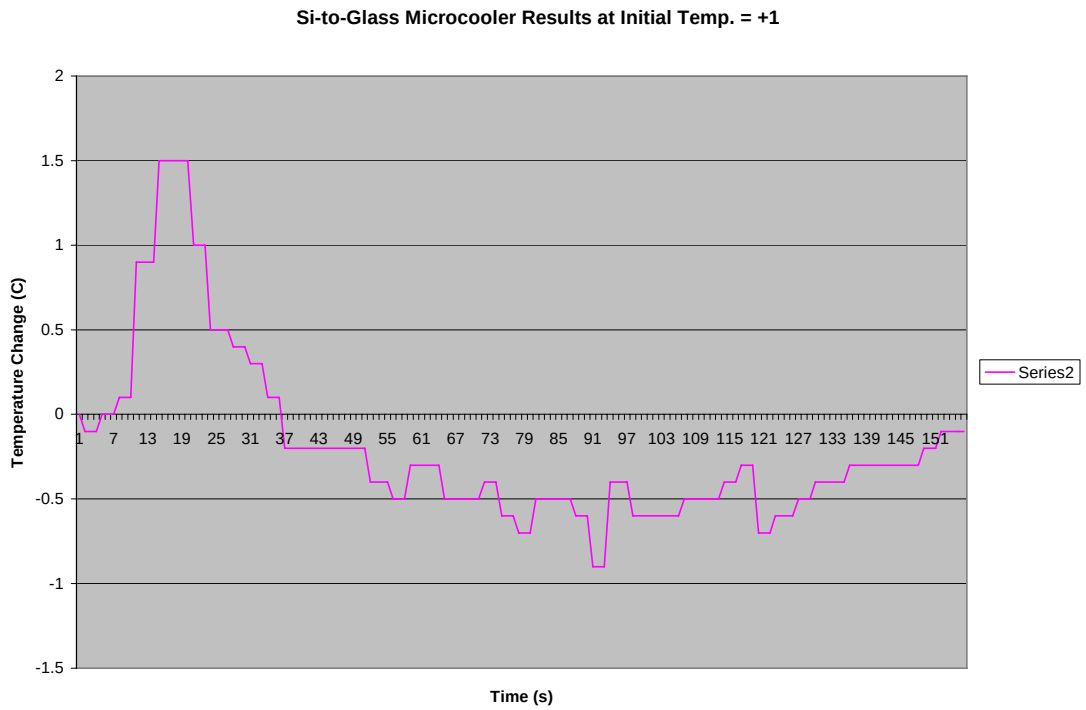

Figure 4.5 Si-to-Glass Microcooler at Initial Temp. of +1 C

Proceeding in the experiment at initial temperature conditions below 0 C (273 K), the MCE provided by the GdSiGe block combined with the heat conduction properties of the Silicon wafer became more evident and result in a larger temperature difference span. More precisely, an increasing cooling effect leading to a maximum temperature difference span of almost -2.5º C was obtained at initial temperature conditions of -3º C as presented in Figure 4.6.

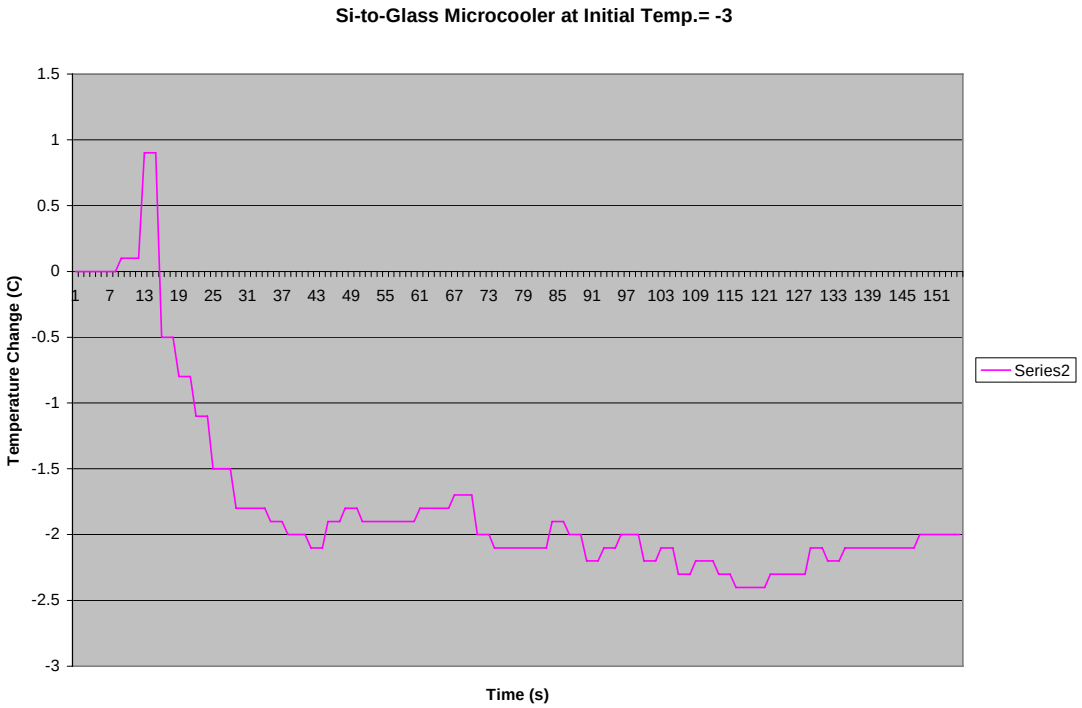

Figure 4.6 Si-to-Glass Microcooler at Initial Temp. of -3^{o} C

Lower initial temperatures (closer to the change of entropy peak value) lead to even better results. Specifically, the microcooler led to cooling effects of over 5º C at initial conditions of approximately -4º C, almost 11º C at initial conditions of about -8º C and 12º C at initial conditions of -11º C. Figures 4.6, 4.7 and 4.8 (below) document the results.

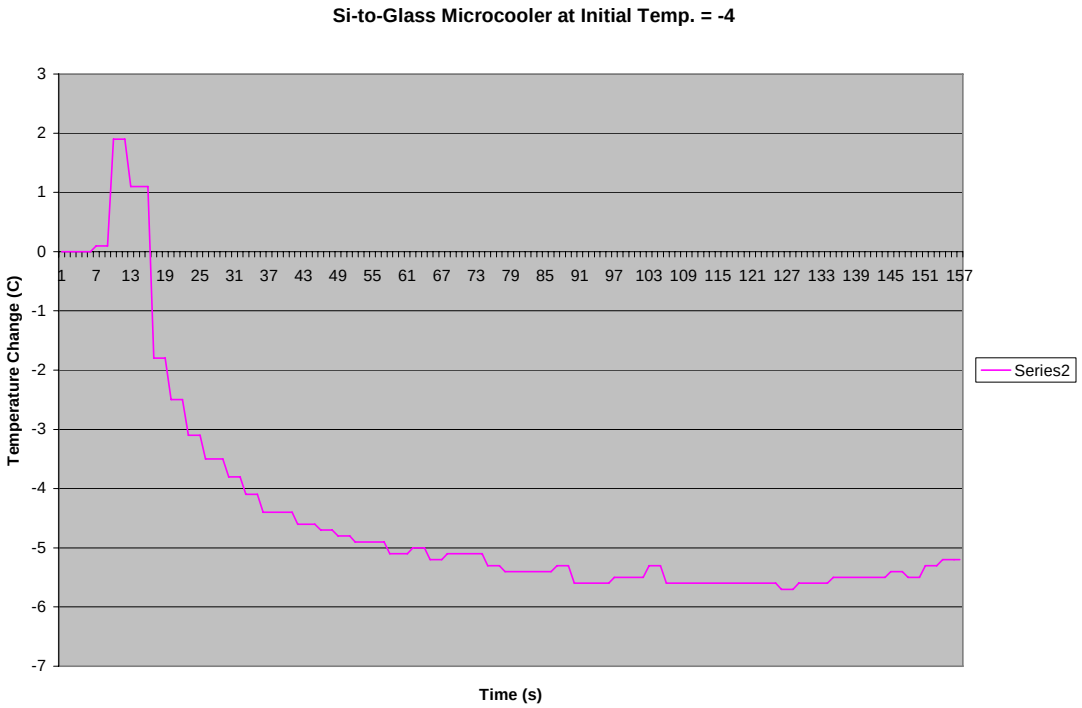

Figure 4.7 Si-to-Glass Microcooler at Initial Temp. of -4^{o} C

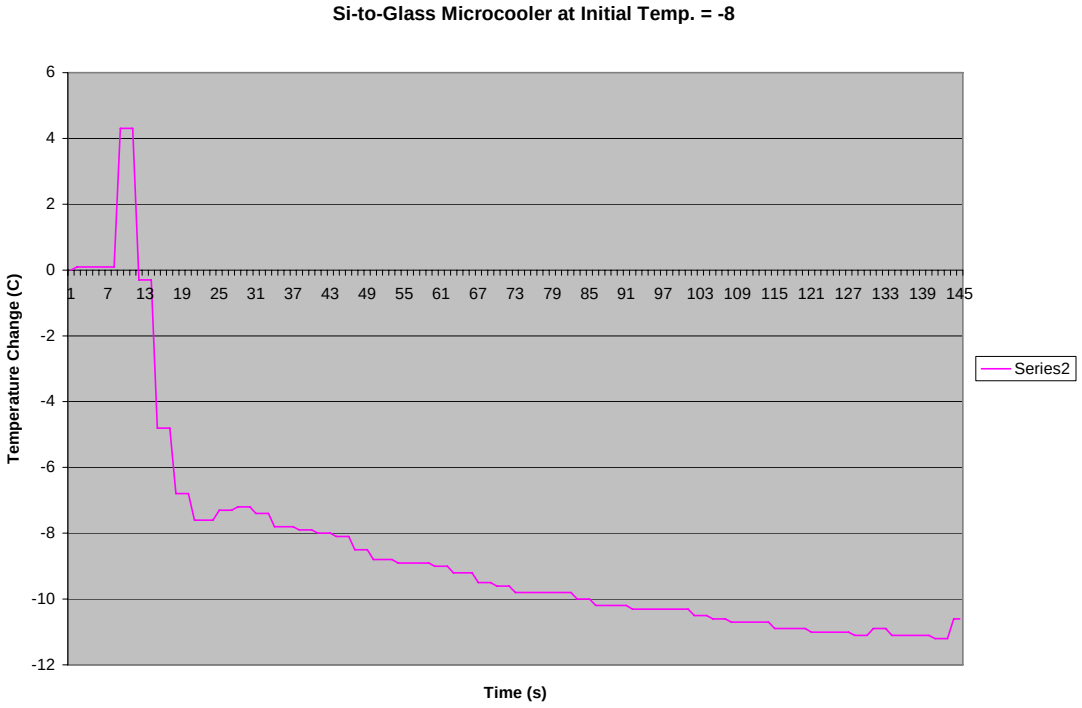

Figure 4.8 Si-to-Glass Microcooler at Initial Temp. of -8^{o} C

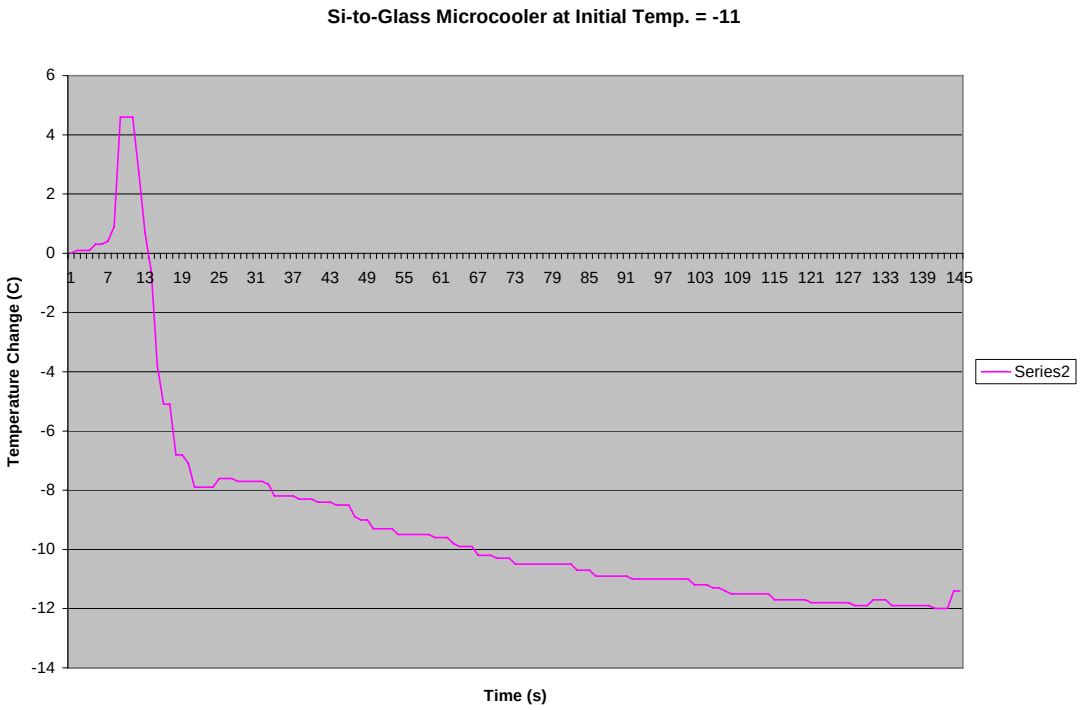

Figure 4.9 Si-to-Glass Microcooler at Initial Temp. of -11^{o} C

4.2.1.1 Si-to-Glass Testing Changing Flow Rate and Interval Time

Further testing was conducted in the Si-to-Glass combination to analyze the effect of flow rate as well as analyzing the role played by the time interval between each cycle. Just like the electro-magnet doesn't instantaneously charge to full magnetic field capacity in the moment it is switched on, once turned off it takes over a minute for it to completely die out. If this standard time is not completely elapsed then the MCE response both in heating and cooling effect is not as efficient as in the previous scenario. Figure 4.10 shows the temperature sensors response versus time in this scenario at an initial system temperature of ~ -11^{o} C and at the same flow rate used before.

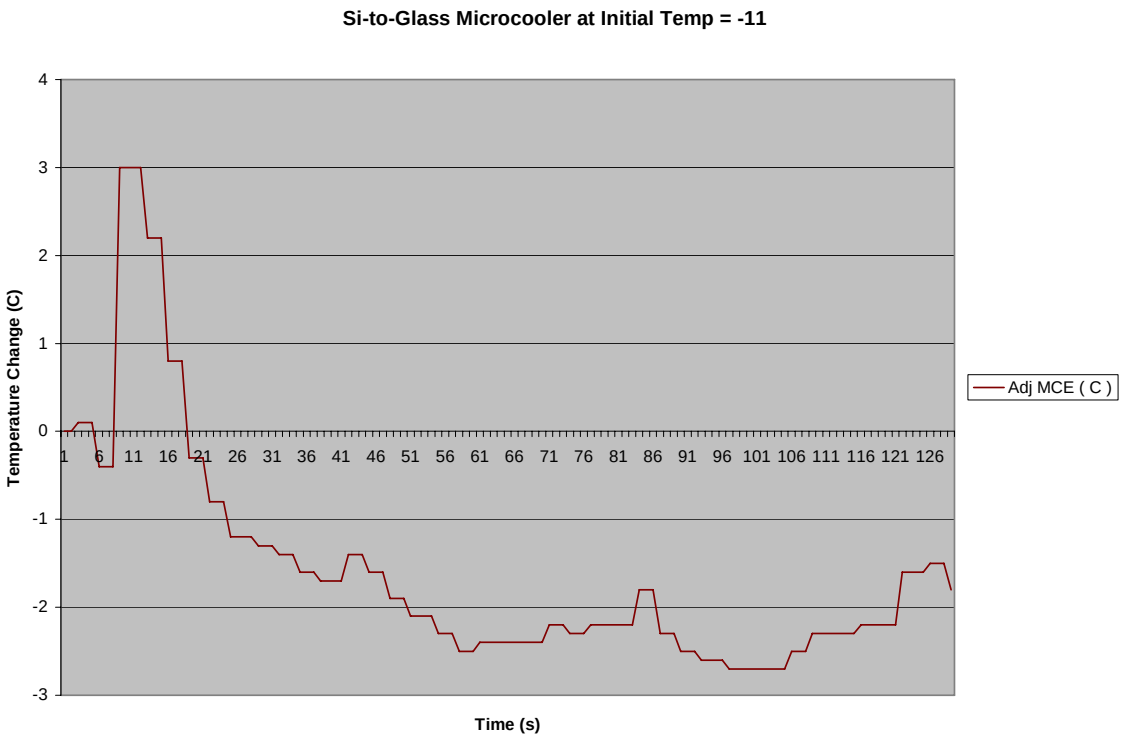

Figure 4.10 Si-to-Glass Microcooler with weak effect

Figure 4.11 shows the effect more closely. The magnet was initially turned on for magnetization and then off for demagnetization. It was then again turned on for magnetization without the necessary standard time elapsed in between and as a result the heating effect was just about half the initial one.

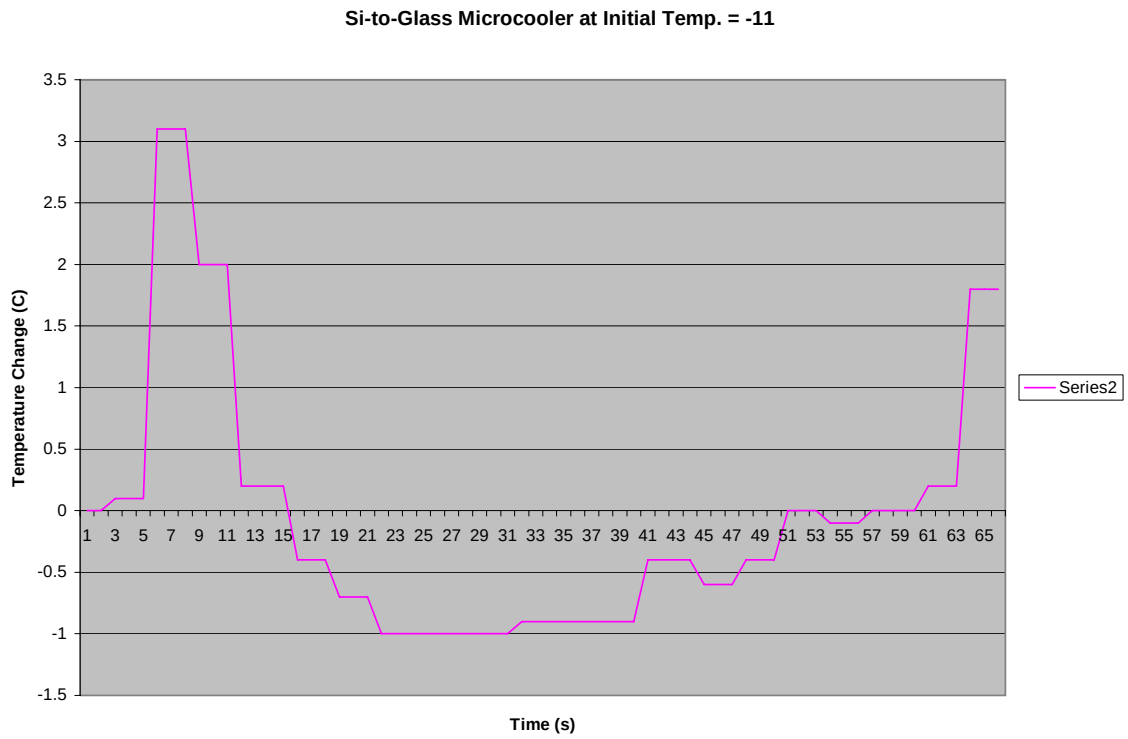

Figure 4.11 Si-to-Glass Microcooler when magnet has not died out

Flow rate was both doubled and halved for previous experiment settings without significant changes in the heating or cooling effect. This is most likely due to working at such small scale. As previously described the MEMS system enhances the surface area to volume ratio, improving the heat transfer between the fluid and the ferromagnetic material and this corresponds to non detectable temperature change within a change in flow rate. A normal size system like the one seen in Chapter 2 would account for changes in liquid flow rate given its much lower surface area to volume ratio.

4.2.2 Results for Silicon-to-Silicon

A final experiment was conducted using the Si-to-Si wafer combination obtained through fusion bonding. A similar procedure was followed. However, this

time the bonding didn't hold for long and approximately after 25 seconds into the testing session there was a leaking between the wafers. Figure 4.10 illustrates the result.

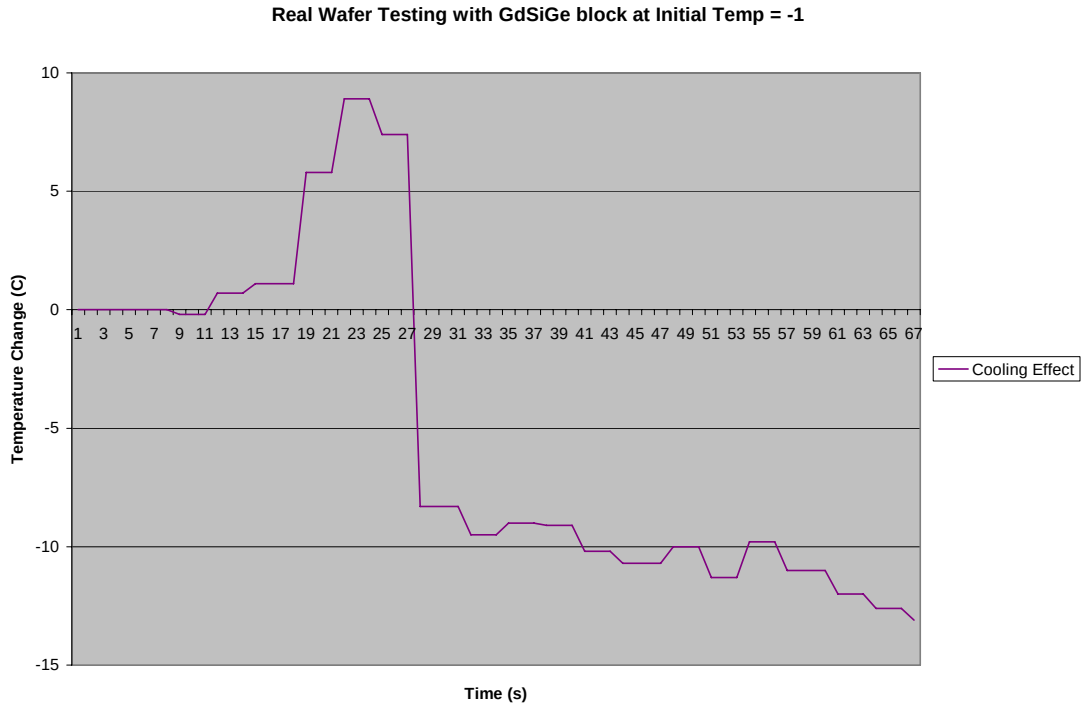

Figure 4.12 Si-to-Si Microcooler at Initial Temp. of -1 C

Before the leaking took place, the heating process seemed to be greatly improved compared to the Glass-to-Si wafer combination even if only at an initial temperature of -1º C (pretty far from the peak of entropy change). This is due to the fact that Glass is not as good of a heating conductor as Silicon. This would predict even better results in the cooling effect and this result opens up exciting avenues for future research.

4.3 Discussion and Future Work

Three different testing procedures were undertaken to analyze the cooling properties of the designed microcooler. The first one involved a Plexiglas wafer from

which only the magnetocaloric properties of GdSiGe were exploited. In the following testing sessions magnetocaloric changes in the fluid were recorded for different initial system temperatures where a Glass-to-Si combination was used. Exploiting the peak of entropy of GdSiGe a remarkable cooling effect of about 12º C was obtained. Even better results are suggested by the third experiment where Si-to-Si combination was adopted, although the process couldn't be fully completed because of leaking in the bonding between etched wafer and bare wafer.

The results are encouraging and suggest that a refrigerator could be constructed using two such microcoolers (magnetocaloric beds) with two heat exchangers, a pump and several valves as shown in Fig. 4.11 [16]. The microcoolers are analogous to the expansion stage and compression stage of a gas refrigeration system.

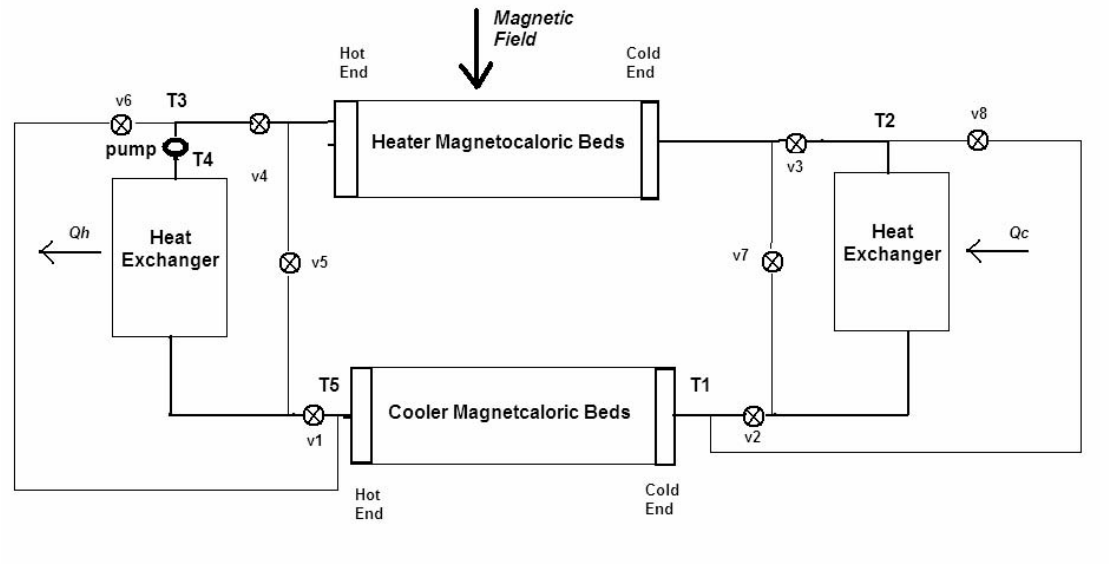

Figure 4.13 Configuration of magnetic refrigerator

CHAPTER 5 CONCLUSION

In this thesis, a MEMS microcooler based on magnetocaloric effect was presented and evaluated. This chapter summarizes the contributions of the thesis and places MEMS microcoolers in the general context of innovation for magnetic refrigeration.

5.1 Contributions

MEMS microcoolers are a significant advance in applications of the magnetocaloric effect (MCE) and magnetic refrigeration. The MEMS microcooler is the first method to effectively applying the MCE of Gd based compounds at relatively low magnetic fields. Testing and results in Chapter 4 showed that this approach is indeed powerful, outperforming traditional magnetic refrigeration that is based on the use of superconducting magnets.

5.2 Conclusion

The exploitation of the magnetocaloric effect, the relative small size of the device, and initial temperature conditions of the system combine to produce a novel methodology for the heating and cooling of fluids without the use of volatile, environmentally hazardous fluids. Not only is this method environmentally friendly, but it supports continual innovation. Thus, this thesis is a first step in optimizing the study of low-energy requirement solutions to the need for liquefaction of hydrogen and household refrigeration.

REFERENCES

[1] E. Cartlidge, “Attractive advance towards magnetic refrigerator,” *Physics World*, Jan. 9, 2002

[2] V.K. Pecharsky, and K.A. Gschneidner, Jr., “Magnetocaloric effect and magnetic refrigeration,” *Journal of Magnetism and Magnetic Materials* 200 (1999) 44-56

[3] S.N. Sambandam, S. Bhansali, and V.R. Bhethanabotla, “Study on magnetocaloric GdSiGe thin films for microcooling applications,” TMS Annual Meeting, Charlotte, NC, March 14-18, 2004

[4] S. C. Kim, B. Bethala, S. Ghirlanda, S. Sambandam, and S. Bhansali, “Design and Fabrication of a Magnetocaloric Microcooler,” *ASME International Mechanical Engineering Congress and Exposition*, IMECE 2005-82720, Orlando, FL, 2005

[5] B. Bethala, “Bulk Silicon Based Temperature Sensor,” *Master’s Thesis*, University of South Florida, Department of Electrical Engineering, October 31, 2005

[6] S.C. Collins, F.J. Zimmermann, *Phys. Rev.* 90 (1953) 991

[7] C.V. Heer, C.B. Barnes, J.C. Daunt, *Rev. Sci. Instr.* 25 (1954) 1088

[8] G.V. Brown, J. *Appl. Phys.* 47 (1975) 3673

[9] W.A. Steyert, J. *Appl. Phys.* 49 (1978) 1216

[10] J.A. Barclay, W.A. Steyert, U.S. Patent No. 4,332,135, June 1, 1982

[11] J.A. Barclay, U.S. Patent No. 4,408,463, October 11, 1983

[12] C. Zimm, A. Jastrab, A. Sternberg, V. Pecharsky, K. Gschneidner, Jr., M. Osborne, and I. Anderson, “Description and performance of a near-room temperature magnetic refrigerator,” *Advances in Cryogenic Engineering*, Vol. 43

[13] Pecharsky, V.K., and Gschneidner Jr, K.A., 1997, “Giant Magnetocaloric Effect in Gd5(Si2Ge2),” *Physical Review Letters*, 78, No. 23, pp. 4494-4497

[14] Tegus, O., Bruck, E.H., Zhang, L., Dagula, W., Buschow, K.H.J., and Boer, F.R. de, 2002, “Magnetic-phase Transitions and Magnetocaloric Effects,” *Physics B*, (319) 174-192

[15] http://www2.polito.it/ricerca/thin-film/Activity/MEMS/anodic_bonding.htm

[16] Rahman, M.M., and Rosario, L., 2004, “Thermodynamic Analysis of Magnetic Refrigerators,” *Proceedings 2004 ASME International Mechanical Engineering Congress and Exposition*, Vol. 3, Anaheim, California

BIBLIOGRAPHY

X. Bohigas, E. Molins, A. Roig, J. Tejada, and X.X. Zhang, "Room-Temperature Magnetic Refrigerator Using Permanent Magnets," *IEEE Transactions on Magnetics,* Vol. 36, No. 3, May 2000

P. Clot, D. Viallet, F. Allab, and A. Kedous-Lebouc, *Member, IEEE*, J.M. Fournier, and J.P. Yonnet, "A Magnet-Based Device for Active Magnetic Regenerative Refrigeration," *IEEE Transactions on Magnetics,* Vol. 39, No. 5, September 2003

A.J. DeGregoria, L.J. Feuling, J.F. Laatach, J.R. Rowe, J.R. Trueblood, and A.A. Wang, "Test Results of an Active Magnetic Regenerative Refrigerator," *Advances in Cryogenic Engineerin*, Vol. 37, Part B

S.J. Lee, J.M. Kenkel, V.K. Pecharsky, and D.C. Jiles, "Permanent Magnet Array for the Magnetic Refrigerator," *Journal of Applied Physics,* Vol. 91, No. 10, 15 May 2002

P. Shirron, E. Canavan, M. DiPirro, M. Jackson, T. King, J. Panek, and J. Tuttle, "A Compact, High-Performance Continuous Magnetic Refrigerator for Space Missions," *Cryogenics* 41 (2002) 789-795